Giant dielectric permittivity of electron-doped manganite thin films, $Ca_{1-x}La_xMnO_3$ $(0 \leqslant x \leqslant 0.03)$

J. L. Cohn[a] and M. Peterca[b]
Department of Physics, University of Miami, Coral Gables, Florida 33124

J. J. Neumeier
Department of Physics, Montana State University, Bozeman, Montana 59717

(Received 14 June 2004; accepted 24 October 2004; published online 30 December 2004)

A giant low-frequency, in-plane dielectric constant, $\epsilon \sim 10^6$, for epitaxial thin films of $Ca_{1-x}La_xMnO_3$ $(x \leqslant 0.03)$ was observed over a broad temperature range, $4\ K \leqslant T \leqslant 300\ K$. This phenomenon is attributed to an internal barrier-layer capacitor (IBLC) structure, with Schottky contacts between semiconducting grains. The room-temperature ϵ increases substantially with electron (La) doping, consistent with a simple model for IBLCs. The measured values of ϵ exceed those of conventional two-phase IBLC materials based on $(Ba,Sr)TiO_3$ as well as on recently discovered $CaCu_3Ti_4O_{12}$ and (Li,Ti)-doped NiO. © *2005 American Institute of Physics*.
[DOI: 10.1063/1.1834976]

I. INTRODUCTION

High-permittivity dielectric materials play an important role in electroceramic devices such as capacitors and memories. Recent reports of giant permittivity have directed considerable attention to several new material systems: nonferroelectric $CaCu_3Ti_4O_{12}$,[1] percolative $BaTiO_3$–Ni composites,[2] and (Li,Ti)-doped NiO.[3] Of particular interest for applications is the weakly temperature-dependent permittivity of these materials near room temperature. The enormous dielectric constant of these materials, $\epsilon \sim 10^5$, appears to be[4] a consequence of an internal barrier-layer capacitor (IBLC) structure, composed of insulating layers between semiconducting grains. IBLCs with effective $\epsilon \sim 10^5$ based on $(BaSr)TiO_3$ are well known,[5] but their usefulness is limited by a strong frequency and temperature dependence of their dielectric constant. Thus the newly discovered materials suggest that increases in ϵ values and/or simplification of processing could yield new and useful IBLC materials.

Here we report on giant values of the effective dielectric constant, $\epsilon \sim 10^6$, observed at low frequencies $(f \leqslant 100\ kHz)$ for thin films of the electron-doped manganite, $Ca_{1-x}La_xMnO_3$ $(0 \leqslant x \leqslant 0.03)$. The large and weakly T- and f-dependent ϵ near room temperature is attributed to an IBLC microstructure, comprising a network of depletion layers between semiconducting grains. ϵ is enhanced by electron doping via La substitution for Ca or oxygen reduction.

II. EXPERIMENTAL METHODS

Polycrystalline targets of $Ca_{1-x}La_xMnO_3$ $(x \leqslant 0.03)$ were prepared by solid-state reaction as described previously.[6] X-ray powder diffraction revealed no secondary phases and iodometric titration, to measure the average Mn valance, indicated an oxygen content for all targets within the range 3.00 ± 0.01. Thin films were grown by pulsed laser deposition using a 248-nm KrF excimer laser, with an energy density of $\sim 0.8-1.2\ J/cm^2$, pulse repetition rate of 10 Hz, and target-substrate distance, 4 cm. The films were deposited on $LaAlO_3$ (LAO) substrates of [100] orientation, with substrate temperature of 750 °C, and oxygen pressure of 200 mTorr. Following the depositions, the chamber was filled to 700-Torr oxygen, held at 500 °C for 30 min, and subsequently cooled to room temperature. Film thicknesses were $\sim 50-170$ nm. X-ray diffraction (XRD) indicated the epitaxial growth of the pseudocubic perovskite for all films, with lattice parameter, $a = 3.72$ Å for $CaMnO_3$. The full widths at half maximum of the (200) film reflections were typically 0.4°. Scanning electron microscopy indicated an average grain size of $0.5-1\ \mu m$.

Impedance measurements were performed with a Hewlett–Packard model 4263B LCR meter in the frequency range 100 Hz–100 kHz. A model HP16034E test fixture was used at room temperature, and a coaxial-lead, four-terminal pair arrangement in a cryostat for low temperatures. Silver paint electrodes, annealed at 300 °C, were applied on opposing edges of the specimens so that the ac voltage (0.2 V for all measurements) was applied in the film plane. In this configuration, the film and substrate capacitances are additive; the equivalent circuit for contacts, film, and substrate is shown in the inset of Fig. 1. A contact capacitance can lead to apparently large values[7] of ϵ and thus great care is required to distinguish the true response of the sample. To address this issue, contact contributions to the impedance were eliminated at room temperature for some films by measuring the length dependence of the impedance (film + substrate), $Z = R + jX$, on a series of films deposited simultaneously onto precut substrates of different lengths, l. Since the contact capacitance and resistance should be independent of l, the measured reactance and resistance should be linear in l, $X = X_0 - \beta l$ and $R = R_0 + \beta' l$, respectively. $X_0 = \omega L - \omega R_C^2 C_C / [1 + (\omega R_C C_C)^2]$ is a constant determined by a small serial inductance, L (also assumed independent of l),[8] and the

[a]Electronic mail: cohn@physics.miami.edu
[b]Present address: Physics Department, University of Pennsylvania, Philadelphia, PA.

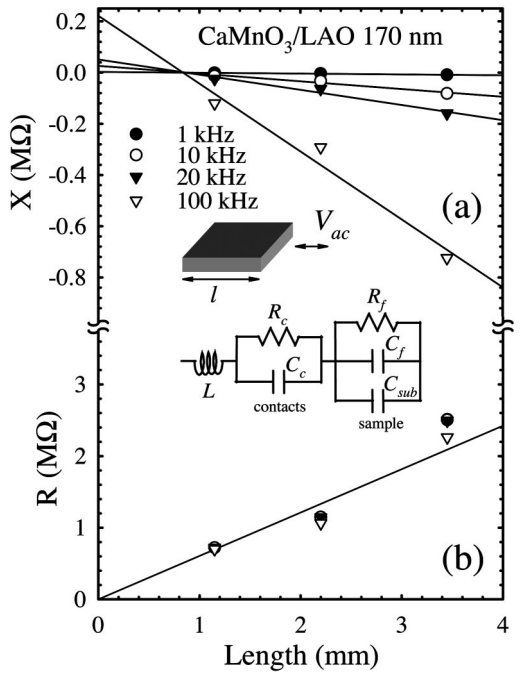

FIG. 1. (a) $X(l)$ and (b) $R(l)$ for a 170-nm $CaMnO_3$/LAO film at room temperature. The inset shows the contact configuration and equivalent circuit.

capacitive reactance of the contacts. These relations are followed well by the raw data (Fig. 1). The dielectric constant of the film was computed as

$$\epsilon_f = \frac{1}{\omega A_f \epsilon_0} \frac{\beta}{\beta^2 + \beta'^2} - \epsilon_{\text{sub}} \frac{A_{\text{sub}}}{A_f}, \tag{1}$$

where $\omega = 2\pi f$ is the angular frequency of the applied voltage, A_f (A_{sub}) is the film (substrate) contact area, and ϵ_{sub} is the substrate dielectric constant. The latter, determined from a similar analysis of $Z(l)$ for blank substrates, was $\epsilon_{\text{sub}} = 24$ in good agreement with published values.[9] Uncertainty in ϵ_f determined from Eq. (1), arising principally from the scatter in the data, was typically ±20%. The values for ϵ_f determined from the length dependence analysis were consistently larger than those determined from direct measurements, indicating a predominance of the inductive reactance over the capacitive reactance of the contacts (i.e., $X_0 > 0$). The $\epsilon(T)$ data presented below from the direct measurements thus underestimate the true magnitude. The uncertainty in ϵ for the direct measurements near room temperature (where $C_f \gg C_{\text{sub}}$) is given by that of the film thickness (±10%). At the lowest temperatures, where $C_f \ll C_{\text{sub}}$, the uncertainty in ϵ is ±50%, largely due to a ±5% uncertainty in C_{sub}. For all measurements, the impedance was independent of ac voltage (50 mV–1 V) and applied dc bias (0–2 V).

III. RESULTS AND DISCUSSION

The impedance of the target materials was measured in separate experiments. $CaMnO_3$ is an antiferromagnetic ($T_N \approx 125$ K) semiconductor with a small electron density associated with native defects, particularly oxygen vacancies, that yield a substantial room-temperature conductivity, $\sigma \sim 100\ \Omega^{-1}\,\text{m}^{-1}$. Electron doping via La substitution for Ca

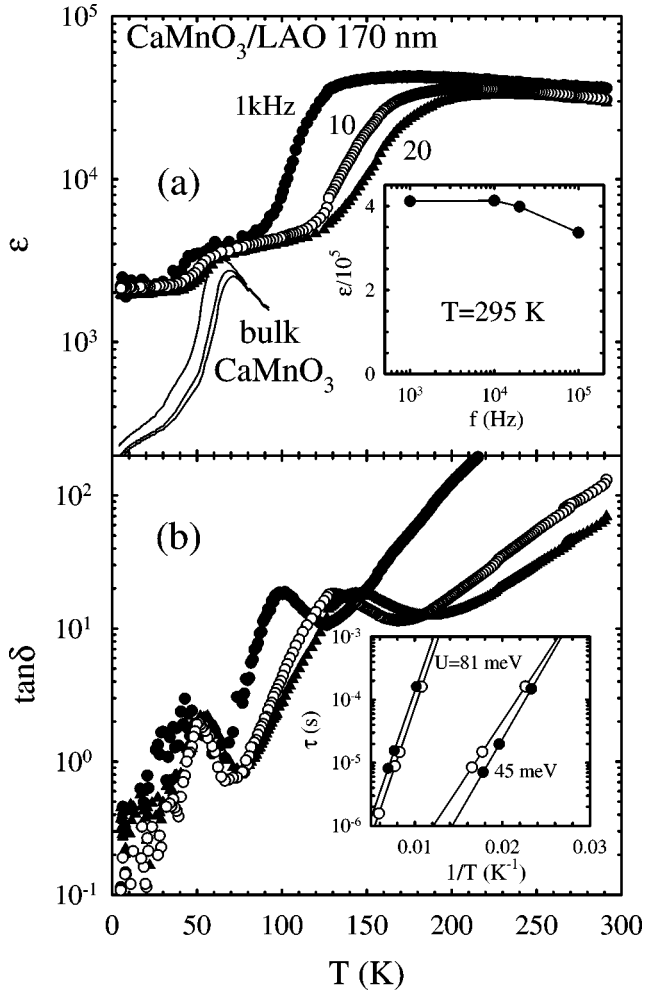

FIG. 2. (a) $\epsilon(T)$ and (b) $\tan\delta(T)$ at three frequencies for a 170-nm $CaMnO_3$/LAO film. The solid curves in (a) are for bulk $CaMnO_3$ at the same frequencies. The inset in (a) shows $\epsilon(f)$ at room temperature for a second piece of the same film. The inset in (b) shows Arrhenius behavior of relaxation times determined from peaks in tan δ for both pieces of the film and corresponding average activation energies.

further enhances σ, especially at low T.[6] ϵ could be determined reliably only at $T \lesssim 100$ K where the capacitive reactance was sufficiently large ($\gtrsim 0.1\ \Omega$). ϵ was described as the sum of a constant term ~25–50 (the high-frequency and lattice terms) and a dipolar contribution associated with hopping charge carriers.[10] The latter gives rise to steps in $\epsilon(T)$ which occur at lower T with decreasing frequency, as shown for $CaMnO_3$ in Fig. 2(a) (solid curves). This indicates a relaxation process associated with thermal activation of localized charge carriers, characterized by a relaxation time, $\tau = \tau_0 \exp(U/k_B T)$. Analyzing the maxima in $d\epsilon/dT$ (corresponding to $\omega\tau = 1$) we find $U = 103$ meV and $\tau_0 = 7.5 \times 10^{-14}$ s. These parameters are typical of polaronic relaxation in $LaMnO_3$ (Ref. 11) and other perovskites.[12] For comparison, $U = 54$ meV, $\tau_0 = 8.4 \times 10^{-10}$ s were reported for single-crystal $CaCu_3Ti_4O_{12}$,[13] and $U = 313$ meV, $\tau_0 = 8.5 \times 10^{-13}$ s for (Li,Ti)-doped NiO.[3] Relevant to the subsequent discussion of films, it was found that increasing the electron density, either through oxygen reduction or La doping, resulted in a decrease (increase) in $U(\tau_0)$. Further details of the measurements on the polycrystalline bulk materials will be presented elsewhere.[14]

Figure 2(a) shows $\epsilon(T)$ at three frequencies ($\leqslant$20 kHz) for a 170-nm film of $CaMnO_3$. The inset shows $\epsilon(f)$ at room temperature for a second piece of the same film measured at 100 kHz. At low temperatures, ϵ has a magnitude comparable to the bulk material and small steps occur at temperatures similar to those at which the bulk material exhibits dipolar relaxation. With increasing temperature a second dispersive step is observed near 200 K, with ϵ increasing by an order of magnitude. For $T>200$ K, $\epsilon \sim 3-4\times10^4$ with weak temperature and frequency dependencies. Both steps in ϵ appear as maxima in the dielectric loss [tan δ, Fig. 2(b)]. The appearance of the high-temperature step is typical of the IBLC materials where insulating barriers separate semiconducting grain interiors. Such a system can be modeled as two *RC* circuits in a series, one for the grain interiors and one for the grain-boundary response.[4] The grain-boundary *RC* time constant, $\tau=R_{gb}C_{gb}$, gives rise to a second relaxation process that is thermally activated via the behavior of R_{gb}. From the temperatures of the maxima in tan δ measured for two pieces of this film we compute [inset, Fig. 2(b)] the average values for activation energies $U=45\pm6$ [81 ± 2] meV and $\tau_0=(1.6\pm1.2)\times10^{-9}$ s [$(9.4\pm3.5)\times10^{-9}$ s] for the grain interior (grain-boundary) relaxations. The values of U and τ_0 inferred for the grain interiors are significantly smaller and larger, respectively, than the corresponding values determined for the targets. This indicates that the grains of the film are more oxygen deficient, and suggests that oxygen is lost during deposition. Consistent with this conclusion, the films have[14] $T_N\approx200$ K in accord with magnetic measurements on oxygen deficient, bulk $CaMnO_{3-\delta}$.[15]

Figure 3 shows $\epsilon(T)$ and tan $\delta(T)$ for a 55-nm film grown from a $Ca_{0.97}La_{0.03}MnO_3$ target. The qualitative features of the data for the as-prepared specimen (open symbols) are similar to that of the $CaMnO_3$ film except that ϵ is substantially larger, $\sim6\times10^5$ at 300 K and the lower temperature step in ϵ is absent. The higher carrier density of the La-doped material suppresses the carrier freeze-out responsible for the low-*T* relaxation to temperatures below our measurement range.[14] A greater dc conductivity is responsible for the sharp increase of tan δ at higher temperatures. The grain-boundary relaxation is evident as weak maxima or plateaus in tan δ. Analysis of the relaxation yields $U=32$ meV and $\tau_0=1.1\times10^{-8}$ s.

After sitting in ambient conditions for three months, ϵ at 300 K for the same specimen (solid symbols) decreased by $\sim20\%-30\%$, but tan δ had decreased dramatically by more than four orders of magnitude at 1 kHz and nearly two orders of magnitude at 100 kHz (Fig. 3). At lower temperatures, tan δ exhibits well-defined maxima, and below these maxima matches the data in the as-prepared state. Thus much of the loss near room temperature in the as-prepared films is associated with dc conduction that is substantially suppressed with "aging."

As for other IBLCs composed of compound semiconductors, our data can be understood by considering the films to be random arrays of close-packed, electrically active semiconducting grains. Boundaries between grains contain an interface charge Q_i, and are adequately described as double Schottky barriers[16] (DSB) with capacitance, $C_{DSB}=\epsilon\epsilon_0A/2x_0$, where A is the area of contact between grains, ϵ is the bulk semiconductor dielectric constant, $x_0=Q_i/2N_0$ is the depletion layer width on either side of the grain boundary (assumed symmetric), and N_0 is the donor density in the bulk semiconducting grains. Since the grain diameter D is typically $\gg x_0$, the "brickwork" model[5] can be applied to the array of grains, such that the effective dielectric constant is given approximately as, $\varepsilon_{eff}\approx(D/2x_0)\epsilon=\epsilon DN_0/Q_i$.

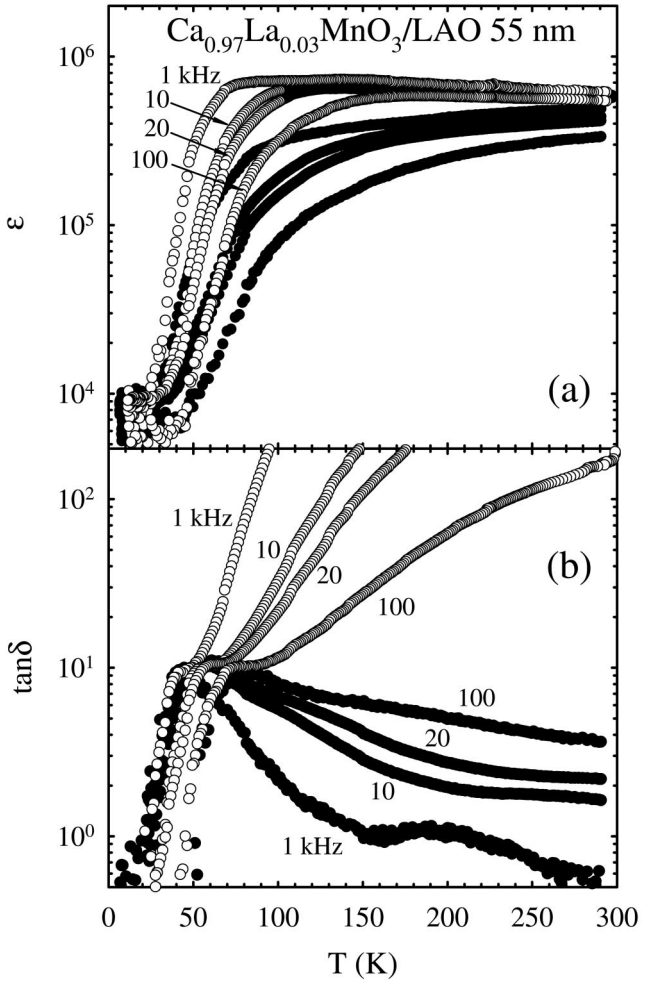

FIG. 3. (a) $\epsilon(T)$ and (b) tan $\delta(T)$ at several frequencies for a 55-nm $Ca_{0.97}La_{0.03}MnO_3$/LAO film, as-prepared (open symbols) and "aged" for three months in air at room temperature (closed symbols).

With increased electron (La) doping, ϵ for the films increases considerably (Fig. 4). These data allow for a test of the simple model above. Reasonably assuming that the oxygen vacancy concentration (y) for the films is independent of x, we compute the slope, $d\epsilon_{eff}/dx$, by making the substitution $N_0=(x+2y)/V_{fu}$,

$$\frac{d\epsilon_{eff}}{dx}=\frac{\epsilon D}{Q_iV_{fu}}, \tag{2}$$

where $V_{fu}=51$ Å^3 is the volume per formula unit.[17] The line in Fig. 4 yields $d\epsilon_{eff}/dx\approx2\times10^7$. Using $\epsilon\sim10^3$ (Fig. 2 and Ref. 14) and $D=0.5$ μm (from scanning electron microscopy), we compute an interface charge density of $Q_i\simeq5\times10^{17}$ m^{-2}. This value is typical of those found for a variety of compound semiconductors.[16] That ϵ_{eff} is approximately

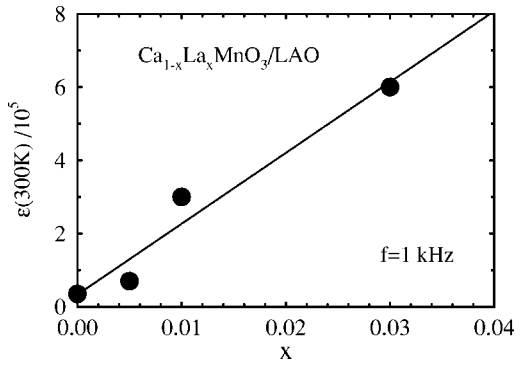

FIG. 4. Doping dependence of the room temperature ϵ at 1 kHz.

linear in x implies that variations in ϵ and Q_i with doping are either negligible or cancel each other.

The aging effect in the films is most likely associated with oxidation at grain surfaces. This hypothesis is supported by preliminary oxygen annealing studies on a 55-nm $CaMnO_3$, (CMO) film. Tan δ was reduced by a factor of 2 with no measurable change in ϵ following a 15-h, flowing-oxygen anneal at 700 °C. A small decrease in ϵ for aged films is consistent with a small increase in Q_i.

Finally, we note that the large values of ϵ reported here are not limited to manganite films with compositions near 100% Ca. We have measured $\epsilon \sim 10^4$ at room temperature for a 55-nm film grown under identical conditions from a $La_{0.7}Ca_{0.3}MnO_3$ target (a colossal magnetoresistance composition). Films of other insulating compositions with the appropriate microstructure may also possess a large effective ϵ.

IV. CONCLUSIONS

In summary, thin films of $Ca_{1-x}La_xMnO_3$ $(0 \leqslant x \leqslant 0.03)$ have been found to exhibit giant low-frequency dielectric constants, $\epsilon \sim 10^6$, that are weakly temperature and frequency dependent near room temperature. These enormous values are attributed to a barrier-layer capacitor microstructure produced during deposition and subsequent exposure to air by oxidation of grain-boundary regions which form an insulating shell on semiconducting grains. ϵ increases with charge-carrier doping, consistent with a reduction in the depletion-layer width at grain-boundary contacts and a nearly doping-independent surface charge. Though lower dielectric losses will be required for applications ($\tan \delta \leqslant 0.05$ is desirable), the considerable reduction of $\tan \delta$ upon aging or oxygen annealing with little decrease in ϵ motivates further investigations of processing conditions.

ACKNOWLEDGMENTS

The authors gratefully acknowledge experimental assistance from Dr. B. Zawilski. The work at the University of Miami was supported, in part, by NSF Grant Nos. DMR-9504213 and DMR-0072276, and at Montana State University by Grant No. DMR-0301166.

[1] M. A. Subramanian, D. Li, N. Duan, B. A. Reisner, and A. W. Sleight, J. Solid State Chem. **151**, 323 (2000); A. P. Ramirez, M. A. Subramanian, M. Gardel, G. Blumberg, D. Li, T. Vogt, and S. M. Shapiro, Solid State Commun. **115**, 217 (2000).
[2] C. Pecharromán, F. Esteban-Betegón, J. F. Bartolomé, S. López-Esteban, and J. S. Miya, Adv. Mater. (Weinheim, Ger.) **13**, 1541 (2001).
[3] J. Wu, C.-W. Nan, Y. Lin, and Y. Deng, Phys. Rev. Lett. **89**, 217601 (2002).
[4] D. C. Sinclair, T. B. Adams, F. D. Morrison, and A. R. West, Appl. Phys. Lett. **80**, 2153 (2002).
[5] C.-F. Yang, Jpn. J. Appl. Phys., Part 1 **36**, 188 (1997).
[6] J. J. Neumeier and J. L. Cohn, Phys. Rev. B **61**, 14319 (2000).
[7] P. Lunkenheimer, V. Bobnar, A. V. Pronin, A. I. Ritus, A. A. Volkov, and A. Loidl, Phys. Rev. B **66**, 052105 (2002).
[8] Any inductance from the film would be expected to scale with l, tending to *reduce* the value of β in Eq. (1); since $\beta \ll \beta'$, the computed dielectric constant represents a lower bound.
[9] See, e.g., *Handbook of Thin Film Devices*, edited by M. H. Francombe (Academic, New York, 2000), Vol. 3, Chap. 1, p. 19.
[10] A. K. Jonscher, *Dielectric Relaxation in Solids* (Chelsea Dielectrics, London, 1983).
[11] A. Seeger, P. Lunkenheimer, J. Hemberger, A. A. Mukhin, V. Yu. Ivanov, A. M. Balbashov, and A. Loidl, J. Phys.: Condens. Matter **11**, 3273 (1999).
[12] O. Bidault, M. Maglione, M. Actis, M. Kchikech, and B. Salce, Phys. Rev. B **52**, 4191 (1995).
[13] C. C. Homes, T. Vogt, S. M. Shapiro, S. Wakimoto, and A. P. Ramirez, Science **293**, 673 (2001).
[14] J. L. Cohn, M. Peterca, and J. J. Neumeier, Phys. Rev. B (in press).
[15] J. Briático, B. Alascio, R. Allub, A. Butera, A. Caneiro, M. T. Causa, and M. Tovar, Phys. Rev. B **53**, 14020 (1996).
[16] F. Greuter and G. Blatter, Semicond. Sci. Technol. **5**, 111 (1990).
[17] C. D. Ling, E. Granado, J. J. Neumeier, J. W. Lynn, and D. N. Argyriou, Phys. Rev. B **68**, 134439 (2003).